Mitigating Methanol Crossover in a Flowing Electrolyte DMFC System

Lucas A. Monteiro1, Pierre L. Moreau2, Giovanni F. Bianchi2, Isabella M. Rossi2, and Alejandro G. Torres2,3*

University of São Paulo, Faculty of Engineering, Mechanical Engineering Department, São Paulo, 05508-010, Brazil

Sorbonne University, Institute of Energy and Climate Research, Paris, 75005, France

Chair for Fuel Cells, University of Barcelona, Spain

Abstract

The flowing electrolyte-direct methanol fuel cell (FE-DMFC) is a type of fuel cell in which a flowing liquid electrolyte is used, in addition to two solid membranes, to reduce methanol crossover. In this study, FE-DMFCs having new materials and design were manufactured and studied. In this design, the flow field plates were made of stainless steel 2205 and had a pin type flow structure. PTFE treated carbon felts were used as the backing layers as well as the flowing electrolyte channel. Nafion® 115 or Nafion® 212 was used as the membranes. The polarization curves and methanol crossover current densities under different methanol concentrations and flow rates of sulfuric acid were measured using fully automated DMFC test stations. The performances of the FE-DMFCs were compared with those of the DMFCs having a single or double membrane. This study is, to the authors' knowledge, the first experimental study on measuring the methanol crossover in a FE-DMFC. The results of this study demonstrate that this technology enables a significant reduction of methanol permeation. At different cell current densities, Faradaic efficiencies up to 98 % were achieved. It was shown that for a fixed flow rate of sulfuric acid solution (5 ml/min), at 0.1 A/cm^2, the Nafion® 115 based FE-DMFC operating at 1 M yields the highest cell voltage (0.38 V). The maximum power density of the FE-DMFC (0.0561 W/cm^2) was achieved when the cell operates with 3 M methanol concentration and 10 ml/min sulfuric acid solution at 0.3 A/cm^2.

Keywords: fuel cell, methanol, DMFC, flowing electrolyte, methanol crossover

1. Introduction

A direct methanol fuel cell (DMFC) is an electrochemical energy conversion technology that is generally used in some portable (e.g. backup power generator [1]), mobility (e.g. range extender [2]), and material handling [3] applications. The main advantages of this technology compared to its competitors, such as the Li-ion battery and the hydrogen fed proton exchange membrane fuel cell, originates from the fuel (liquid methanol) that is used. Methanol is easy to access, store, distribute, and has a high energy density (6100 Wh/kg at 25 °C [4]). In addition, a conventional DMFC can operate at low operating temperature ranges (up to 80 °C), which is advantageous to achieve fast start-up and shut-down periods. The main challenge associated with the wide usage of this technology is mainly due to its low performance and costly materials (e.g. catalysts such as Pt or Pt-Ru). The main reasons for the low DMFC performance can be listed as follows [4]: slow anode and cathode reaction kinetics, water management at the cathode, and methanol crossover.

Methanol crossover, which is the transport of methanol from the anode to cathode, lowers both the electrical efficiency and power density of a DMFC. This process occurs because water is required to be present inside the membrane in order to facilitate the transport of protons through the membrane [5]. Since the properties of methanol are very similar to those of water, methanol can also enter and penetrate the membrane. The primary driving forces for the permeation of methanol are diffusion (caused by the concentration gradient of methanol between the anode and the cathode) and the so-called electroosmotic drag, describing the fact that each proton traversing the membrane is accompanied by a certain number of solvent molecules [6]. These solvent molecules are water and methanol in the relative quantities as they can be found on the anode. Methanol arriving to the cathode is oxidized and wasted without being converted into electricity. During this process methanol and intermediates of its oxidation reaction, like CO, are adsorbed on the cathode catalyst. Therefore, compared to a hydrogen fuel cell, a significantly higher cathode catalyst loading is required in order to have enough reactive sites available for oxygen reduction. In addition, this phenomenon causes a significant voltage drop even under the open circuit voltage (OCV) condition [7].

In order to reduce the negative effects of methanol crossover, different materials and manufacturing techniques have been proposed. These can be divided into three strategies: i) A different polymer than the standard material Nafion® can be used to reduce methanol permeation. ii) Alternatively a polymer, generally Nafion® can be blended with other materials in order to reduce permeation or iii) a barrier layer can be applied onto one or both surfaces of the membrane to prevent methanol from crossing it. To form a barrier layer, sulfonic acid groups can be removed from the surface of the membrane by plasma etching, as shown by Walker et al [8]. Choi et al. [9] used plasma etching and palladium-sputtering on a commercial Nafion® membrane. They found that methanol crossover reduces as the membrane's surface is roughened after applying plasma etching; and the palladium-sputtering decreases this crossover even more. Lin et al. [10] showed that graphene oxide can be used as a barrier layer against methanol oxidation while Holmes at al [11] proposed single layer graphene and hexagonal boron nitride for the same purpose. To follow the second strategy, Ponce et al [12] succeeded in reducing methanol permeation by blending heteropolyacid into a sulfonated PEK-membrane. Kim et al. [13] modified a Nafion® membrane by impregnating the membrane with Pd nanophases. This modification showed lower methanol permeability and a comparable proton conductivity to commercial Nafion® membrane. Recently, some research groups have developed membranes with low methanol permeation and high proton conductivity. Parthiban et al. [14] synthesized a hybrid membrane in which sulfonic acid functionalized graphene was impregnated into a Nafion® matrix; and obtained superior performance than pristine recast Nafion® membrane based DMFCs, as this hybrid membrane reduces methanol permeation and increases proton conductivity.

To follow the strategy of using a different polymer, it is important to have an understanding of how proton conduction works in Nafion® and similar membranes. Gierke at al concluded from SAXS studies that connected pores for channels where the protons are transported in the presence of water [15]. This model was refined by Kreuer to a bicontinuous phase model [16], and showing that a phase separation on a smaller scale will lead to lower methanol permeation than a phase separation on a larger scale. To achieve this, Li et al. [17] synthesized several multiblock copolymer membranes and compared the performance of DMFCs based on these membranes against the performance of commercial Nafion® membranes. They

found that tetramethyl bisphenol A based multiblock copolymer has the properties of the lowest water uptake and methanol permeability; and yields the highest performance for DMFCs. A large number of different sulfonated polymers were suggested to reduce methanol permeation. Besides the fluorinated polymers, often aromatic polymers were suggested in order to avoid oxidation of the C-H bonds under the operating conditions of fuel cells. A list of all these polymers is beyond the scope of this paper. Early reviews were published by Kerres [18] and Kreuer [16]. A recent overview of membrane research activities for DMFC was given by Lufrano et al. [19]. They concluded that perfluorosulfonuc acid membrane based DMFCs yield higher power densities; whereas sulfonated aromatic polymers enable lower methanol permeation and cost.

An alternative way of reducing or eliminating methanol crossover is to use the flowing electrolyte concept. In this concept, instead of a full MEA, two half-MEAs are fabricated and placed on either side of a porous structure (also called flowing electrolyte channel). A fluid (e.g. sulfuric acid solution) having high proton conductivity flows through this channel and sweeps away the methanol crossing over to the cathode. This type of a fuel cell is known as a Flowing Electrolyte-Direct Methanol Fuel Cell (FE-DMFC). This fuel cell is illustrated in Fig. 1. Some numerical and experimental studies were conducted for the development of FE-DMFC. Kordesch and his co-workers initially proposed this concept [20, 21]. Schaffer et al. [22] investigated different spacers used as flowing electrolyte channels (FEC) such as SiC-foams, sintered glass elements made of DURAN® (Schott Glas), a polypropylene fleece of FOAMAX®, a fabric of woven PTFE, a polypropylene grid, and a grid of polyvinylidenediflouride (PVdF). They selected the PVdF fabric as they achieved the highest flow rate with this material. Kjeang et al. [23] developed a computational fluid dynamics (CFD) model to simulate methanol crossover by convection-diffusion mechanisms in the FE-DMFC channel; and studied the effect of various electrolyte channel orientations. The results of their simulations showed that the counter flow channel orientation minimizes the methanol crossover. Colpan et al. [24, 25] developed 1D and 2D single phase models of the FE-DMFC. In these studies, they investigated the effect of recirculation of the methanol leaving the FEC to the inlet of the anode as well as several operating parameters such as velocity of methanol, air and sulfuric acid solution, FEC thickness, and methanol concentration. They showed that higher performance could be achieved by taking the FEC thickness as low as possible, the FEC and cathode inlet flow rates high enough, and by recirculating the sulfuric acid solution. Kablou et al. [26] built a short stack for FE-DMFC and showed that the stack could be operated without any significant degradation in the performance at high methanol concentrations. Duivesteyn et al. [27, 28] developed 3D isothermal and non-isothermal FE-DMFC models for the improvement of the porous structure of the FEC design. Sabet-Sharghi et al. [29] studied the effect of sulfuric acid concentration, electrolyte flow rate, and flowing electrolyte channel thickness on the performance of a FE-DMFC experimentally. They concluded that 0.6 mm channel thickness and 2 M sulfuric acid concentration should be preferred for better performance. Ouellette et al. [30-33] developed several comprehensive 1D single and two-phase FE-DMFC models and conducted experimental research on alternative liquid electrolytes (e.g. formic acid) for circulating FE-DMFCs. Atacan et al. [34] developed a 2D multiphase non-isothermal model of a FE-DMFC and found that if the inlet temperatures of the anode or cathode is too low, possible flooding could occur within the air channel.

The literature survey conducted shows that there is limited number of experimental studies on FE-DMFCs. In these studies, no methanol crossover measurements were done experimentally. In the current study, it is aimed to show that methanol permeation can actually be reduced and the performance of a FE-DMFC can be improved using a new cell design and materials. To achieve this goal, the performances of FE-DMFCs built using different membranes (Nafion® 115 or Nafion® 212) were evaluated under different methanol concentrations (0.5 M, 0.75 M, 1 M, and 3 M). The performances of the FE-DMFCs were compared to those of DMFCs having a single or double membrane. DMFCs having a double membrane were manufactured in this study to make a fairer comparison between the DMFC and FE-DMFC. In addition, the effect of the flow rate of sulfuric acid solution on the performance and crossover current density of FE-DMFC was assessed.
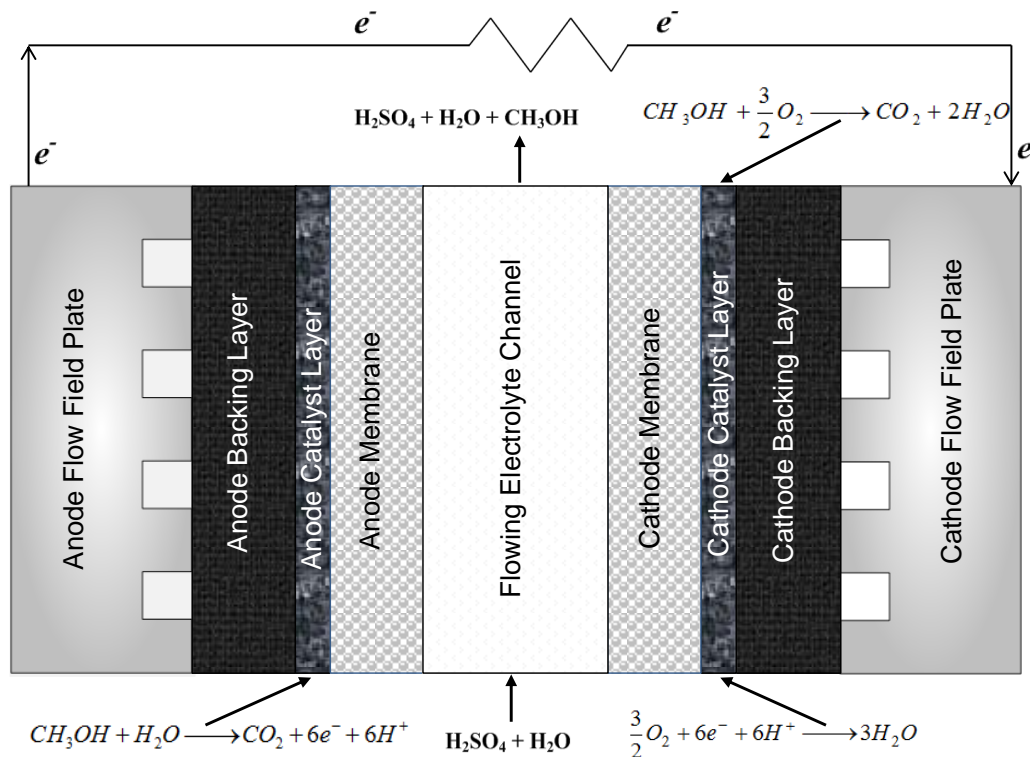

Fig. 1. A schematic of a Flowing Electrolyte-Direct Methanol Fuel Cell (FE-DMFC).

2. Experimental

2.1 End plate and flow field design

For both the DMFC and FE-DMFC, the flow field was designed as a grid type (or checker board type) with dimensions of 1 mm for the width and depth of the channels as well as width of the lands. The active surface area of the MEA was taken as 42×42 mm². The DMFC single cells were designed in such a way that the end plates (stainless steel 316Ti) and the flow field plates (graphite) are separate pieces. In the FE-DMFC, these components were one piece, and composed of stainless steel 2205 (SS 2205), due to its comparatively higher corrosion resistance to sulfuric acid than other commonly used stainless steel types

[35,36]. As a definition, if the corrosion rate is less than 0.1 mm/year, the corrosion resistance is considered good [35]. Figure 2 shows the isocorrosion curves for SS 2205, which were obtained from two different sources [35,36]. As can be seen from this figure, for a temperature of 70 °C (the operating temperature of the fuel cell in this study), this material has a good corrosion resistance for a sulfuric acid concentration up to 1.23 M (11.5 wt%) and 1.85 M (16.7 wt%) according to Refs. [35,36], respectively. On the other hand, Fig. 2 also shows that the proton conductivity of sulfuric acid is highest when the sulfuric acid concentration is taken as 4.2 M. At this peak point, the corresponding value of the conductivity is 132.4 S/m [37]. However, considering the longevity of the cell, the FE-DMFC was tested at a 2 M sulfuric acid concentration. In this case, the conductivity of sulfuric acid (98.5 S/m) will be close to its peak value and the corrosion rate will only be slightly higher than 0.1 mm/year.
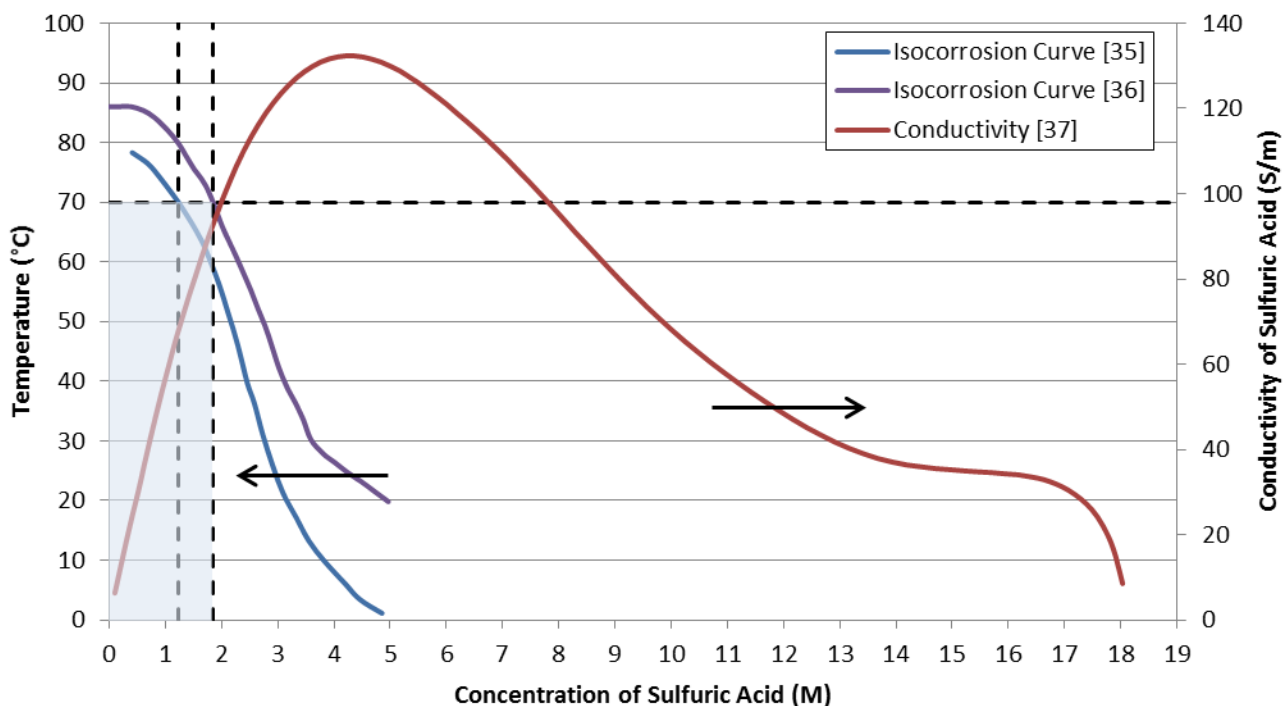

Fig. 2. Isocorrosion curve (0.1 mm/year) for stainless steel 2205 (left y-axis) and the change of proton conductivity of sulfuric acid at 70 °C (right y-axis) with respect to its concentration.

2.2 Catalyst ink preparation

To prepare the catalyst ink for the anode, appropriate amounts of Pt-Ru/C (HiSPEC® 12100 by Johnson Matthey), ultrapure water (18.2 MΩ·cm), 15 % Nafion® solution (LQ-1115 by Ion Power) and alcohol (1-propanol and 2-propanol mixture with 75 % and 25 % volume ratio, respectively) were added to a small glass vessel consecutively. After adding the ultrapure water, the wetted catalyst was mixed for 30 seconds using a shaker (IKA® MS 3 Basic). The final mixture was mixed under pulse mode of 0.4 s ON and 0.6 s OFF at an amplitude of 30 % for 2 minutes using 3 mm microtip (MS73) in an ultrasonic mixer (Bandelin SONOPULS HD 3200). The procedure for preparing the cathode ink was similar. However, Pt/C (HiSPEC® 9100 by Johnson Matthey) was used as the catalyst in the ink formulation. The Nafion® contents (the ratio

of the weight of dry Nafion® to the total weight of dry contents in the catalyst) of the anode and cathode were taken as 0.26 and 0.2, respectively.

2.3 Catalyst coated membrane manufacturing

The catalyst coated membranes were prepared using the decal transfer method. Firstly, an anode mask (anti-static UV adhesive film by Ultron Systems, Inc.), which has an opening with the size of the active area, was placed on a decal substrate (Thomaplast fiberglass cloth coated with PTFE, type RCT-NRN-SP700). This assembly was placed on the automatic film applicator (Erichsen 509) and the catalyst ink was coated on to the decal substrate using the knife coating method. A similar procedure was applied to prepare the catalyst coated substrate for the cathode side. The anode and cathode catalyst coated substrates were then dried overnight at room temperature and put in an oven at 60 °C for 1 hour the next day. The electrodes were then transferred to the Nafion® 115 (N115) or Nafion® 212 (N212) membranes by hot pressing. The conditions for hot pressing were as follows: 3 mins at 130 °C and 0.5 kN/cm^2 for N115, and 3 mins at 150 °C and 1 kN/cm^2 for N212.

Using the methods described above, both sides coated membranes (to be used in DMFCs having single membrane) and single side coated membranes (to be used in either DMFCs having double membranes or FE-DMFCs) were manufactured. The single side coated anode and cathode membranes were hot pressed at 130 °C and 0.5 kN/cm^2 for 3 mins to produce the catalyst coated DMFC having double membrane. The catalyst loadings for anode and cathode were 2.7 mg$_{Pt-Ru}$/cm^2 for anode and 1.8 mg$_{Pt}$/cm^2 for cathode.

2.4 Cell assembly

For assembling a DMFC, the catalyst coated membrane was placed between the flow fields and two 200 μm thick PTFE gaskets (one placed on either side of the MEA). A PTFE impregnated carbon felt (Freudenberg H2315 I6) and a carbon felt with a PTFE microporous layer (Freudenberg H2315 CX312) were used as the anode and cathode backing layers, respectively. After the cell was closed, the screw bolts were tightened with 5 N·m torque to achieve the necessary compression inside the cell. For the FE-DMFC, carbon felt (Freudenberg H2315 I6), which has a thickness of 0.175 mm, was placed between the anode and cathode half-MEAs. This was used for the FEC. The sealing of the FE-DMFC was achieved with two 0.25 mm gaskets in contact with the flow fields, two 0.1 mm gaskets behind the single side coated membranes to seal the flow fields, and another 0.25 mm gasket to seal the FEC. A schematic of the assembly of the FE-DMFC is shown in Fig. 3.
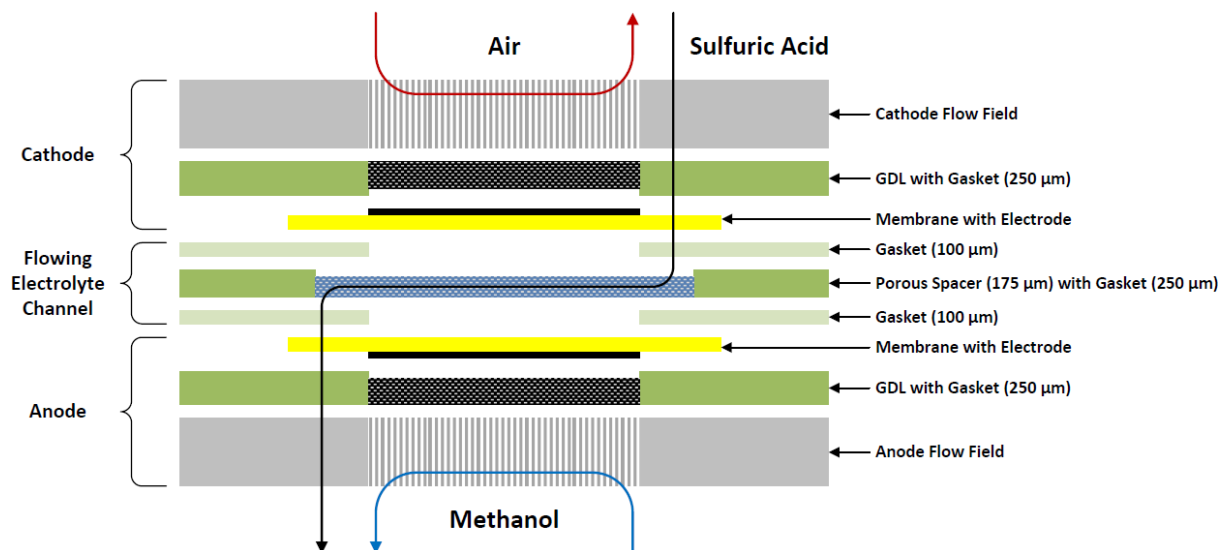
Fig. 3. Schematic of the FE-DMFC assembly.

2.5 Single cell testing

After assembling the cells and performing leakage tests, the single cell was placed in the fuel cell test station, which was built in Forschungszentrum Jülich. The fuel cell test station mainly consists of a peristaltic pump (for feeding methanol solution), a micro-flow controller (for feeding air), a load bank (to control current density), heater cartridges (to adjust the temperature of the feeding lines and the cell), a condenser at the cathode outlet (to convert any condensable gases into liquid), and a CO_2 sensor built on top of the condenser (to measure the CO_2 concentration and thus to calculate the methanol crossover rate). The test station is fully automated and can be controlled by a custom software developed in LabVIEW. This test station has the capability of conducting the break-in and performance tests for the prescribed conditions as well as measuring the methanol permeation. During the break-in stage, the fuel cell was first run in the following conditions for three times: OCV (one hour) and then between 0 and 0.3 A/cm^2 with a step size of 0.02 A/cm^2 (3 minutes for each step). This procedure was then repeated four more times with a cooling step (OCV at 35 °C for 2 hours) between each repetition. If the cell voltage corresponding to a current density was less than 0.1 V, the test station skipped to the next cycle automatically (not to damage the catalysts). To measure the methanol permeation, CO_2 generated at the cathode side was measured by a CO_2 sensor (after correcting for the CO_2 found in the compressed air); and it was established that the molar flow rate of methanol permeation is equal to that of the CO_2 generated. All measurements were taken every 10 seconds and then the averages of the values of the desired parameters (e.g. cell voltage and CO_2 concentration) were taken. The tests were performed at 70 °C and 1 atm with 36.9 $ml/(cm^2·min)$ of dry air and 0.22 $ml/(cm^2·min)$ of diluted methanol solution (0.5 M, 0.75 M, 1 M or 3 M). The current density was changed between 0 to 0.3 A/cm^2 with a step size of 0.02 A/cm^2 and 0.06 A/cm^2 for the cell voltage and methanol permeation measurements, respectively. For the FE-DMFC tests, 2 M sulfuric acid was pumped with a flow rate of 5 ml/min for the baseline conditions. This flow rate was also set to 1 ml/min and 10 ml/min for specific cases discussed in Section 3.4. The total Ohmic resistance of the cell was measured using electrochemical impedance spectroscopy by changing the frequency between 100 kHz and 250 mHz for a given condition. The change of frequency with the

magnitude of the impedance and the phase angle were shown on the same diagram (i.e.: Bode Diagram). The frequency corresponding to the 0° phase angle and the magnitude of the impedance at that frequency were recorded. This point corresponds to the fuel cell's Ohmic resistance . Since both the catalyst coating and the performance measurements were done using automated equipment and well established procedures, the reproducibility of the results were high (within ±5% range).

3. Results and Discussion

3.1. Effect of Membrane Arrangement

Three different MEAs based on N115 membranes were manufactured to assess the effect of membrane arrangement on the performance of the fuel cell at two different methanol concentrations (0.5 M and 3 M). These arrangements are as follows: a conventional DMFC having a single membrane (S-DMFC), a DMFC having a double membrane (D-DMFC), and a FE-DMFC. The experiments were run at the same conditions as discussed in Section 2.5. The results for the polarization curve and the change of crossover current density with respect to cell current density for 0.5 M and 3 M are shown in Figs. 4 and 5, respectively. As can be seen in Fig. 4a, when the cell is operating at 0.5 M and at a current density of 0.1 A/cm^2, the cell voltage for the S-DMFC, D-DMFC and FE-DMFC are 0.466 V, 0.417 V, and 0.343 V, respectively. The lower Ohmic resistance of the S-DMFC configuration, due to the considerably shorter path for proton transfer from the anode to cathode is considered to be the main reason for its superior performance. When the membrane thickness is doubled, the Ohmic resistance due to the proton transfer through the membrane increases but the methanol crossover from the anode to the cathode decreases. Fig. 4b shows that the crossover current density decreases from 0.039 A/cm^2 to 0.025 A/cm^2 at a cell current density of 0.1 A/cm^2 when a D-DMFC is used instead of S-DMFC. Because of the lower methanol crossover rate, the OCV for D-DMFC gets also higher as shown in Fig. 4a (0.698 V and 0.737 V for S-DMFC and D-DMFC, respectively). These results show that as the performance gain due to lower methanol crossover is less than the performance loss due to higher Ohmic loss, the overall performance drops when a double membrane is used in a DMFC instead of a single membrane. The limiting current density for a DMFC with a thicker membrane also decreases as expected as can be seen in Fig. 4a. Please note that although the limiting current densities are not shown on the figures in this study (as the minimum recorded cell voltage was taken as 0.1 V), a comparison between the limiting current densities could be made, by considering the location of the point where the Ohmic polarization dominated linear region ends and mass transfer limitations start to dominate.

In the case of the FE-DMFC, in addition to two N115 membranes (with thickness of 2×127 μm), the protons need to pass through a 0.175 mm thick FEC filled with a flowing sulfuric acid solution. The effect of this additional layer on the performance can be estimated as follows. The proton conductivity of a N115 membrane is 17.88 S/m at 70 °C [31]; whereas that of a FEC (with a porosity of 0.78) filled with 2 M H_2SO_4 at 70 °C can be approximated as 67.86 S/m (= 98.5×$0.78^{1.5}$) using the Bruggeman correlation [31]. Hence, the area specific resistance (ASR) only due to the proton transfer through the membrane (including the FEC for FE-DMFC), which is the ratio between the membrane thickness and the proton conductivity of the membrane, can be approximated as 0.071 Ω·cm^2, 0.142 Ω·cm^2, and 0.168 Ω·cm^2 for S-DMFC, D-DMFC, and FE-DMFC, respectively. It was found experimentally (as discussed in Section 2.5) that the ASR for the

S-DMFC, D-DMFC, and FE-DMFC are 0.295 $\Omega \cdot cm^2$, 0.362 $\Omega \cdot cm^2$, and 0.411 $\Omega \cdot cm^2$, respectively. When the difference in the resistances between S-DMFC and D-DMFC as well as D-DMFC and FE-DMFC for both ASR of the membrane (including FEC for FE-DMFC) and the cell are compared, it can be considered that the contribution of the total contact resistances for FE-DMFC to the total Ohmic resistance of the cell is higher than that for the D-DMFC. This difference could be attributed to the different cell designs used for these two different fuel cells. These results also show that the main contribution to the total Ohmic polarization of the cell is due to the hindered proton transfer within the catalyst layers, due to the lower electrolyte volume fraction, as well as the total contact resistances rather than the proton transfer in the membrane (and FEC for FE-DMFC). On the other hand, Fig. 4a shows that the OCV for the FE-DMFC (0.754 V) is higher than both the S-DMFC and D-DMFC. In addition, Fig. 4b shows that the methanol crossover effect in FE-DMFC is very small compared to the other fuel cells. It can be seen from this figure that when the cell current density is 0.1 A/cm^2, the crossover current density for FE-DMFC is 0.002 A/cm^2, which is around ten times lower than that for D-DMFC. This crossover current density corresponds to a Faradaic efficiency of 98 % for FE-DMFC. Here, Faradaic efficiency is defined as the ratio of the cell current density to the summation of the cell current density and the crossover current density. Hence, it can be interpreted that the main reason of the lower performance of the FE-DMFC compared to the D-DMFC is due to the higher Ohmic polarization, in spite of the fact that the FE-DMFC almost eliminates the negative effects of methanol crossover at the cathode. The FE-DMFC also has the lowest limiting current density mainly due to the higher Ohmic resistance and potentially higher water crossover to the cathode. In addition, H_2SO_4 might have an effect on the catalytic reactions at the electrodes.

When 3 M methanol concentration is used instead of 0.5 M, it can be seen from Fig. 5a that the performance difference between the D-DMFC and FE-DMFC is smaller; although the D-DMFC still yields better performance. For this condition, the OCV for the S-DMFC, D-DMFC, and FE-DMFC were measured as 0.683 V, 0.712 V, and 0.690 V. In addition, at 0.1 A/cm^2, the cell voltage was found to be 0.447 V, 0.378 V, and 0.345 V for the S-DMFC, D-DMFC, and FE-DMFC, respectively. The main reason for the decrease in the performance between D-DMFC and FE-DMFC for this current density may be explained as follows. Using higher methanol concentrations in the feed stream causes higher methanol crossover for a DMFC. As FE-DMFC is capable of removing the unwanted methanol crossover, it is less affected with this fact as compared to D-DMFC. In addition, as it can be seen in Fig. 5b, at 0.1 A/cm^2, the crossover current density for D-DMFC and FE-DMFC is 0.277 A/cm^2 and 0.024 A/cm^2; which shows that the increase in the crossover current density is higher in D-DMFC than that in FE-DMFC when 3 M methanol is used instead of 0.5 M. In this case, more than 90 % of permeation was eliminated by the FE-DMFC. The effect of methanol concentration on the performance of these fuel cells is discussed more in detail in Section 3.3.
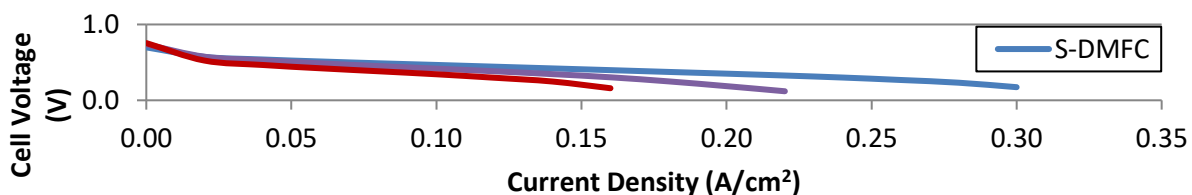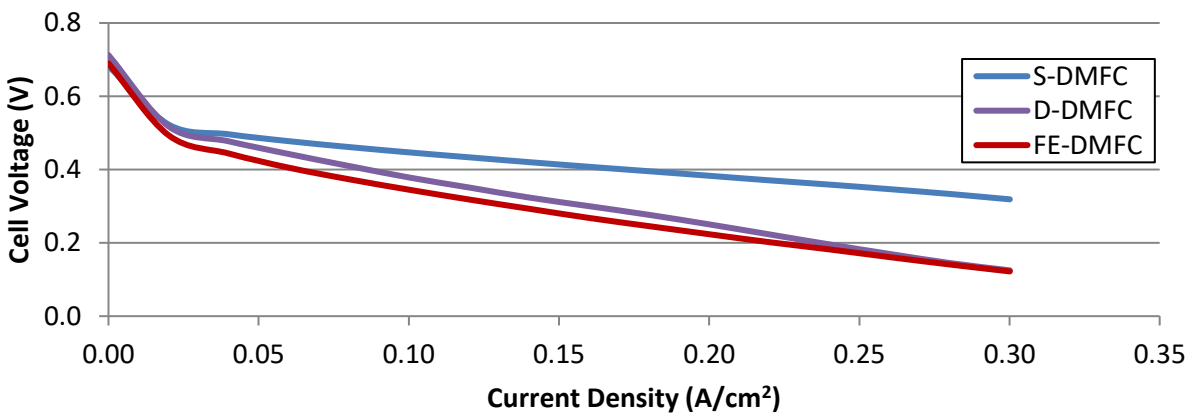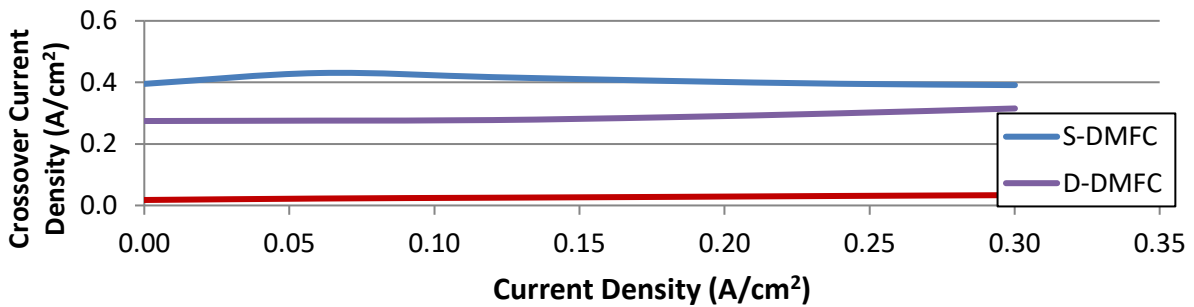

(a)
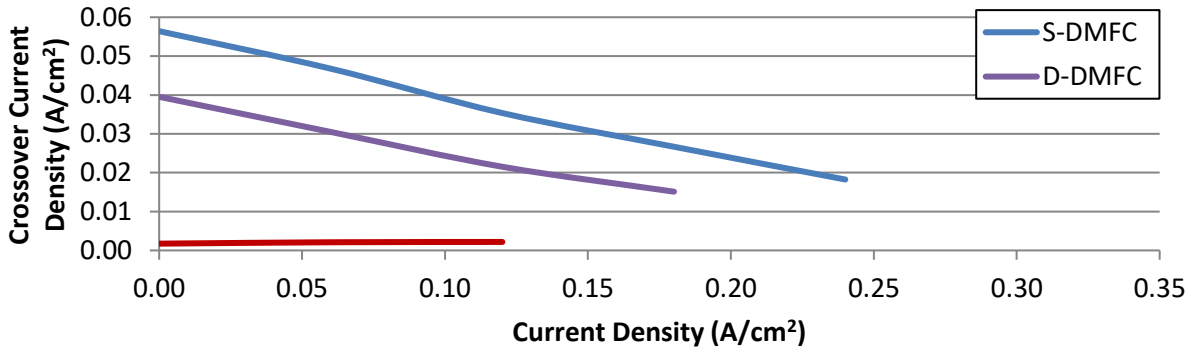
(b)

Fig. 4. (a) Polarization curve and (b) crossover current density of different N115 membrane arrangements (DMFCs having single and double membranes and FE-DMFC) at 0.5 M.


(a)

(b)

Fig. 5. (a) Polarization curve and (b) crossover current density of different N115 membrane arrangements (DMFCs having single and double membranes and FE-DMFC) at 3 M.

3.2. Effect of Membrane Type

In a conventional DMFC, the major contributions to the voltage drop at any current density are the kinetic losses at the anode and cathode electrodes. At low current density conditions, these losses as well as the losses due to methanol crossover are the main reasons of the low performance. In general, as the current density increases, the losses due to electrode and electrolyte resistances increase; and the losses due to mass transport limitations also become more influential [4]. Hence, it is generally desirable to have a membrane with high proton conductivity and low methanol permeability to decrease the Ohmic loss in the membrane and the voltage loss due to the mixed voltage at the cathode. In addition, as the Ohmic polarization is directly proportional to the thickness of the membrane, thinner membranes, in addition to the above mentioned features would be ideal for obtaining better performance. N115 and N212, which are the membranes produced by the same company (DuPont^{TM}) with different thicknesses (127 μm for N115 and 50.8 μm for N212) are commonly used in a DMFC and there are many studies (e.g. [38-40]) on the performance of DMFCs based on these membranes in the literature. Unlike the studies found in the literature, the performance of D-DMFC and FE-DMFC that are based on these membranes and operating at different methanol concentrations are assessed; and the results are presented in this section.

Figures 6a and 6b show the polarization curve and crossover current density for the D-DMFC based on N115 or N212 membrane at 0.5 M and 3 M. When the results obtained at 0.5 M are compared, it can be seen from Fig. 6a that the D-DMFC with a N115 has better performance only at low current density conditions (<0.04 A/cm^2). This is mainly due to the fact that the OCV is generally higher for thicker membranes as methanol permeation is lower for this kind of membranes. The OCV for the D-DMFC using a N115 and N212 are measured to be 0.737 V and 0.681 V, respectively. When Fig. 6b is observed, at this methanol concentration, D-DMFC with a N212 has a higher crossover current density than the D-DMFC with a N115 for any cell current density. Thus a higher voltage loss occurred due to methanol crossover, as expected. For example, at 0.1 A/cm^2, the crossover current density is 0.025 A/cm^2 and 0.066 A/cm^2 for a D-DMFC having N115 and N212, respectively. These results show that the performance loss due to the negative effects of methanol crossover is less than the performance gain due to the increase in the Ohmic polarization when N212 is used instead of N115. At 3 M, the D-DMFC with a N115 seems to operate with a better performance at the low and high current density regions; whereas the D-DMFC with a N212 has a still slightly higher performance between 0.14 A/cm^2 − 0.24 A/cm^2. The improvement in the DMFC performance with a N115 can be explained as follows. By increasing the methanol concentration from 0.5 M to 3 M, the limiting current density increases significantly for the N115 due to the greater availability of reactants as can be seen in Fig. 6a. However, in doing so, the performance loss due to methanol crossover becomes more influential for the N212, as can be seen in Fig. 6b. This is primarily attributed to the higher diffusive flux, and lower mass transfer resistance, across the thinner membrane.

The effect of membrane type on the performance of the FE-DMFC at a methanol concentration of 0.5 M and 3 M is also studied; and the results are shown in Fig. 7. For the FE-DMFCs operating at a low methanol concentration (0.5 M), the trends in the performances of the fuel cells having N115 and N212 membranes seem to be a little different than D-DMFC. For example, Fig. 7a shows that when the methanol concentration is 0.5 M, the OCVs for a FE-DMFC having N115 and N212 are 0.754 V and 0.618 V, respectively. It can be speculated that the lower OCV for FE-DMFC having N212 compared to D-DMFC having N212 can be associated with higher water crossover; thus the cathode might have been flooded with water, hindering the transport of oxygen to the platinum reaction sites. As the reversible cell voltage is a function of the concentration of oxygen reaching the cathode catalyst, the reduced oxygen concentration due to the mass transfer limitations would decrease the OCV. In addition, the limiting current density would also decrease because of the increase in these limitations. In spite of this phenomenon, the FE-DMFC having a N212 still obtained better performance than that having a N115 when the cell current density is higher than 0.08 A/cm^2. For example, at 0.1 A/cm^2, the cell voltages for FE-DMFC having N115 and N212 are 0.343 V and 0.351 V, respectively. Figure 7b shows that the methanol crossover rates for both fuel cells are comparatively low. However, it is still higher for a FE-DMFC having N212 for the given sulfuric acid flow rate (5 ml/min). For example, at the cell current density of 0.1 A/cm^2, the crossover current density is 0.002 A/cm^2 and 0.017 A/cm^2 for FE-DMFC having N115 and N212, respectively. This finding shows that there is more potential for performance improvement for FE-DMFC having N212; which could be achieved by increasing the flow rate of sulfuric acid. This effect is discussed in detail in Section 3.4. When the methanol concentration is selected as 3 M, the trends for the performance of the fuel cells seem to be similar to those operating at 0.5 M. In other words, the FE-DMFC having a N115 has a higher OCV; whereas the FE-DMFC having a N212 has a higher limiting current density. It can also be observed from Fig. 7a that both of the FE-DMFC operating at either 0.5 M or 3 M yields similar performance at 0.1 A/cm^2.

(a)
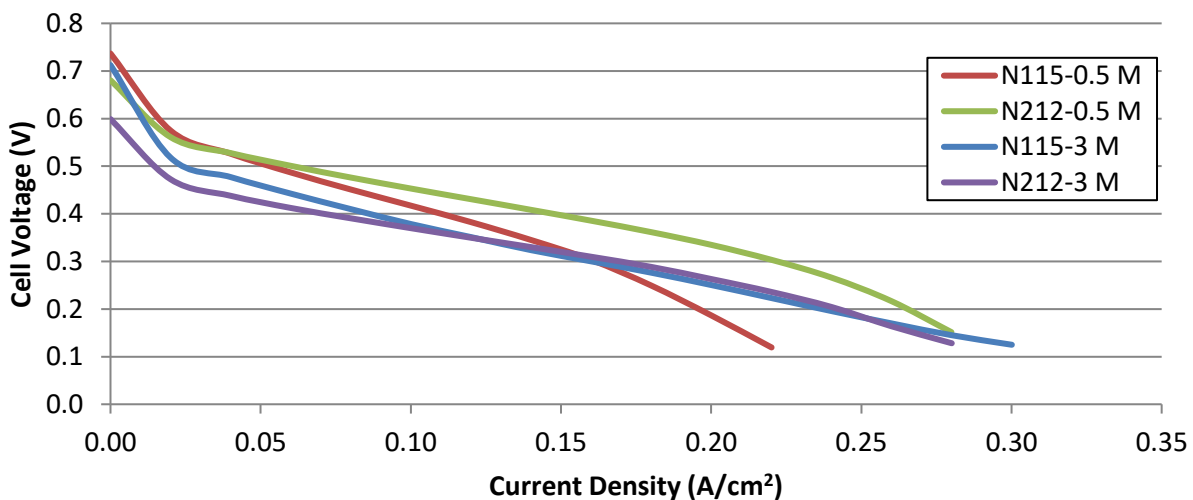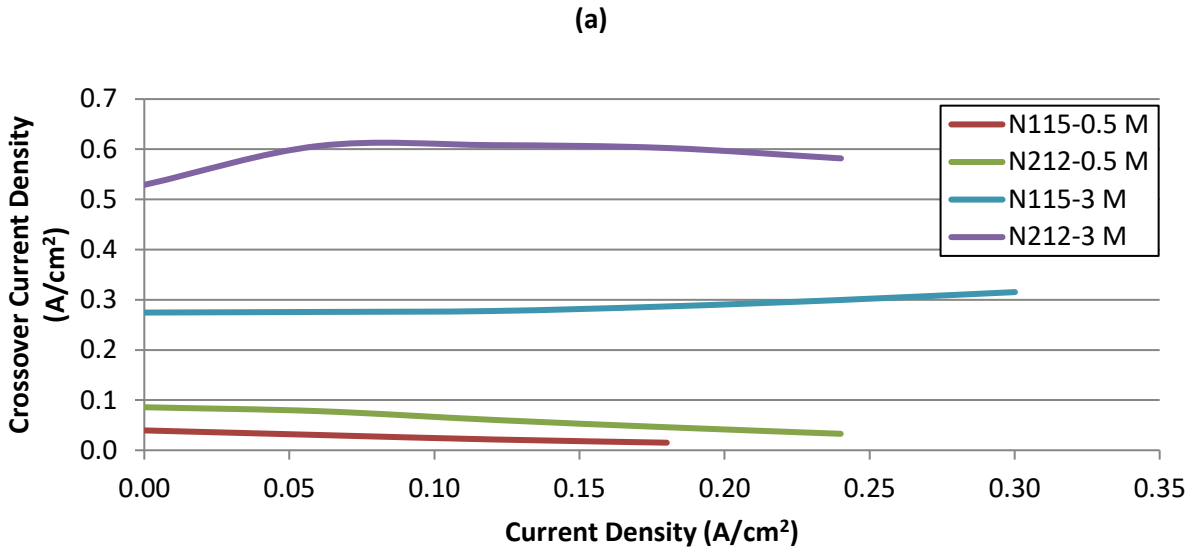
(b)

Fig. 6. (a) Polarization curve and (b) crossover current density of DMFC having a double N115 or N212 membrane at 0.5 M and 3 M.
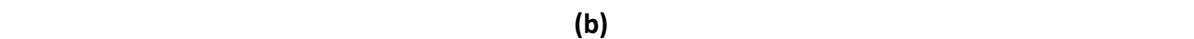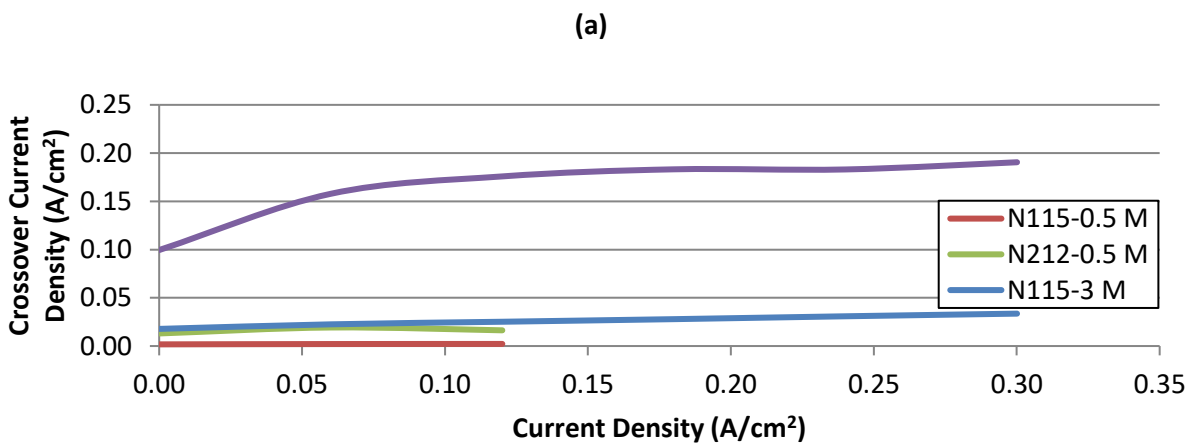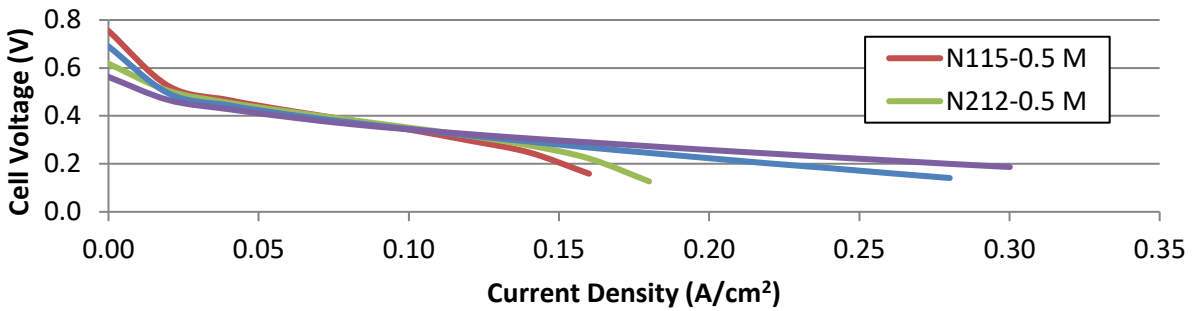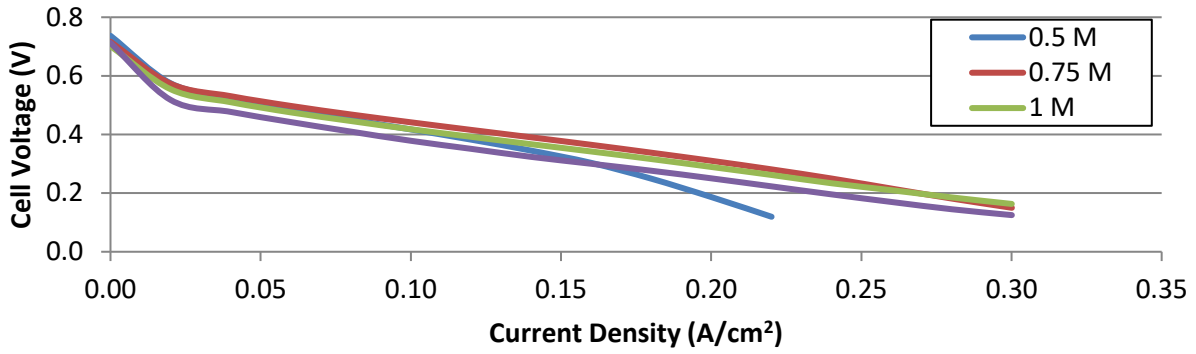

(a)

(b)

Fig. 7. (a) Polarization curve and (b) crossover current density of FE-DMFC based on N115 or N212 membranes at 0.5 M and 3 M.
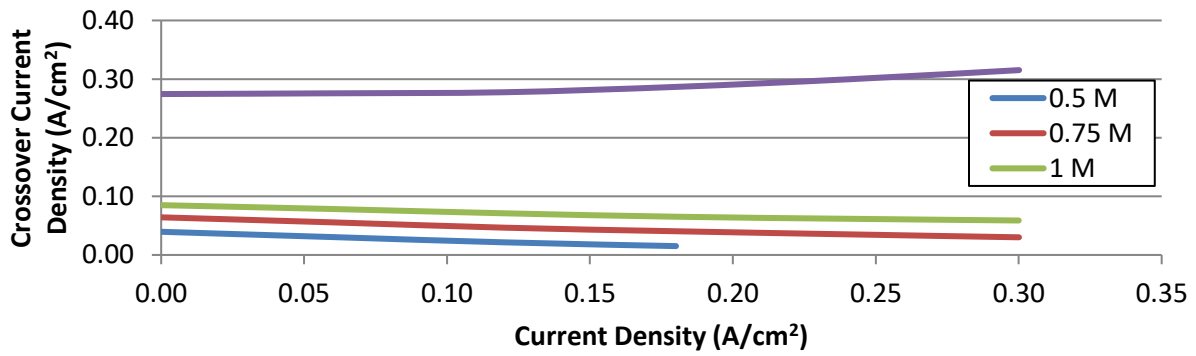
3.3. Effect of Methanol Concentration

Methanol concentration is a critical parameter that affects the performance of a DMFC. It is known that low values of methanol concentration yield lower methanol crossover rates, which in turn increases the OCV. However, limiting current densities also reduce due to the voltage losses due to the increase in the mass transport limitations [4]. In this study, four different values of methanol concentrations (0.5 M, 0.75 M, 1 M, and 3 M) are taken to assess the effect of this parameter on the performance of both the D-DMFC and FE-DMFC. The cell voltages of the D-DMFC and FE-DMFC at 0.1 A/cm^2 are shown in Table 1 for different methanol concentrations for both of the studied membranes. The polarization curve and crossover current density for D-DMFC and FE-DMFC having N115 membrane are shown in Figs. 8 and 9, respectively; and those having N212 membrane are shown in Figs. 10 and 11, respectively. When these figures are observed, the trends for the changes of OCV and crossover current density with respect to the change in methanol concentration are as expected for all cases in general. However, the value of the methanol concentration that yields the best performance change for each case. Figures 8a-11a show that for the wide range of current density, 0.5 M and 0.75 M gave the best performance for a D-DMFC having N212 and N115, respectively, whereas 1 M gave the best performance for a FE-DMFC having N212 and N115. It should be noted that at some of the low and high current density regions, other values of methanol concentration might give higher performance. These results show that, mainly due to the crossover current density reduction in FE-DMFCs, higher methanol concentrations (1 M instead of 0.75 M for N115 case and 1 M instead of 0.5 M for N212 case) gave better performance. As discussed in Section 3.4., even higher methanol concentrations might give higher performances for FE-DMFCs if the flow rate of sulfuric acid solution is adjusted well. These findings show that FE-DMFC has a potential to be used with higher methanol concentrations as compared to DMFC technology.

Table 1. Comparison of the cell voltages between the D-DMFC and FE-DMFC at 0.1 A/cm^2 for different methanol concentrations and sulfuric acid flow rates (for FE-DMFC only)

|	N115					N212				
	0.5 M	0.75 M	1 M	3M		0.5 M	0.75 M	1 M	3M	
D-DMFC	0.42 V	0.44 V	0.42 V	0.38 V		0.45 M	0.44 V	0.44 V	0.37 V	
FE-DMFC	0.34 V (for 5 ml/min H$_2$SO$_4$)	0.37 V (for 5 ml/min H$_2$SO$_4$)	0.38 V (for 5 ml/min H$_2$SO$_4$)	**1 ml/min**	0.31 V	0.35 V (for 5 ml/min H$_2$SO$_4$)	0.36 V (for 5 ml/min H$_2$SO$_4$)	0.37 V (for 5 ml/min H$_2$SO$_4$)	**1 ml/min**	0.29 V
				5 ml/min	0.35 V				**5 ml/min**	0.34 V
				10 ml/min	0.36 V				**10 ml/min**	0.35 V

(a)

(b)

Fig. 8. (a) Polarization curve and (b) crossover current density of DMFC having a double N115 membrane at different methanol concentrations (0.5 M, 0.75 M, 1 M, and 3 M).
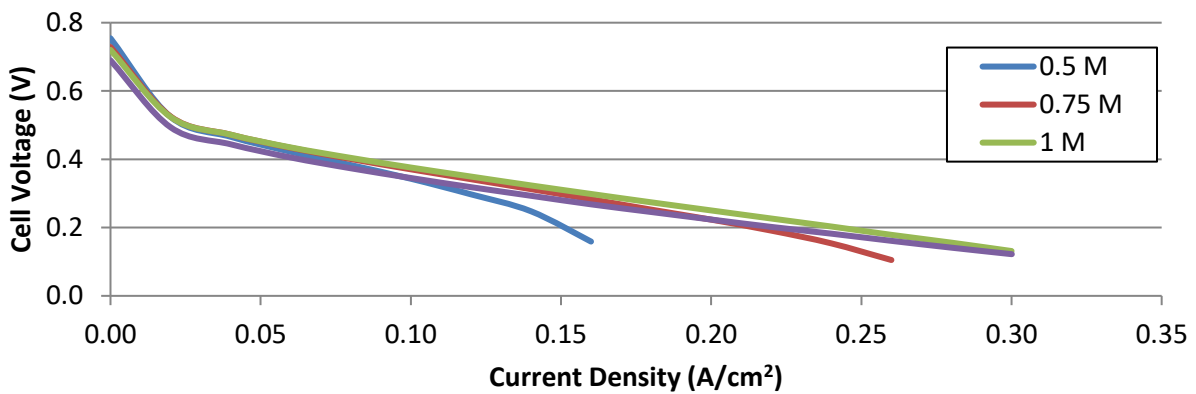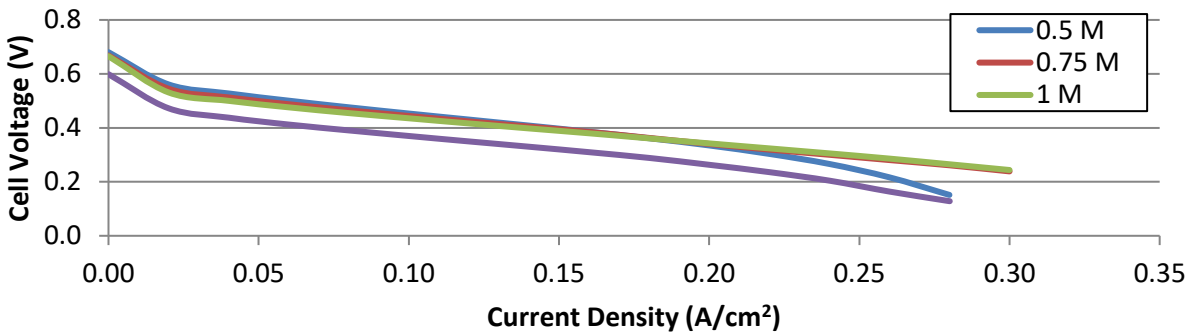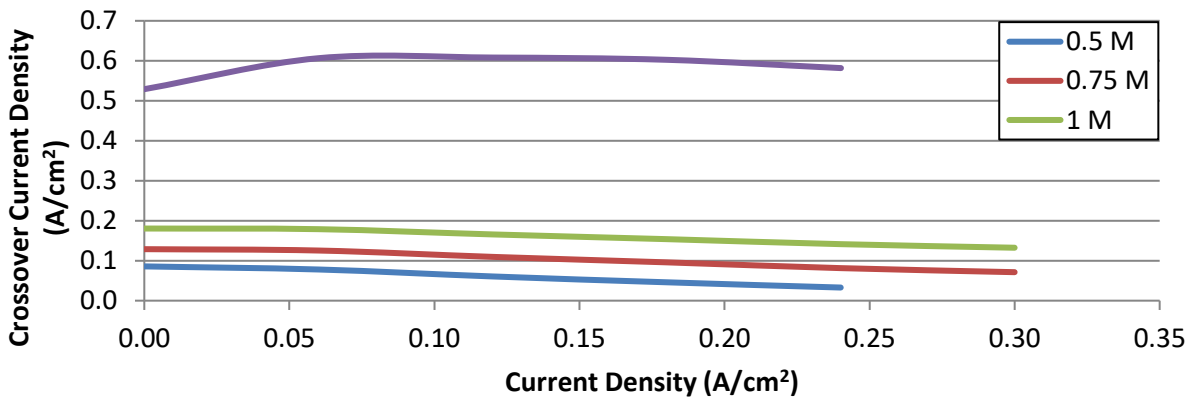

(a)
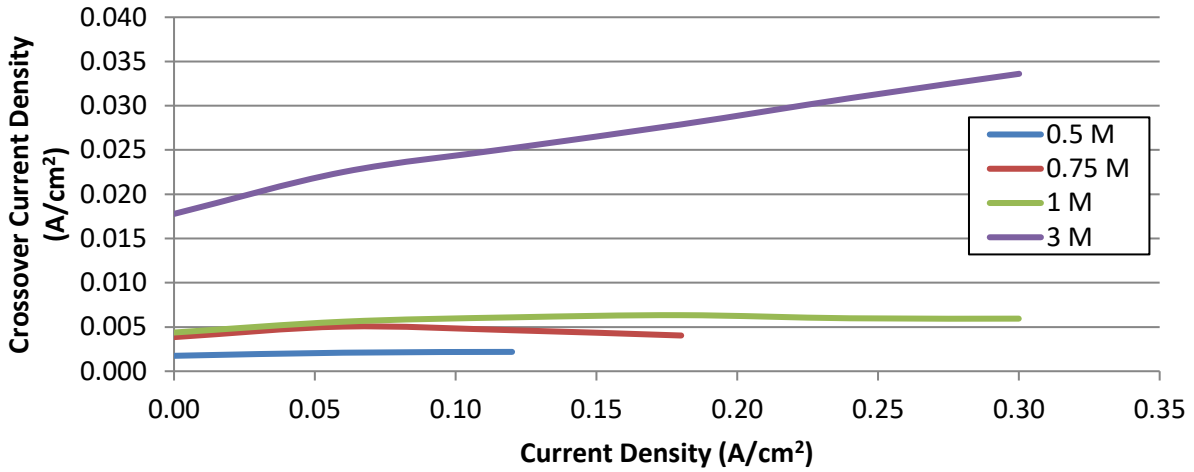
(b)

Fig. 9. (a) Polarization curve and (b) crossover current density of FE-DMFC based on N115 membranes at different methanol concentrations (0.5 M, 0.75 M, 1 M, and 3 M).
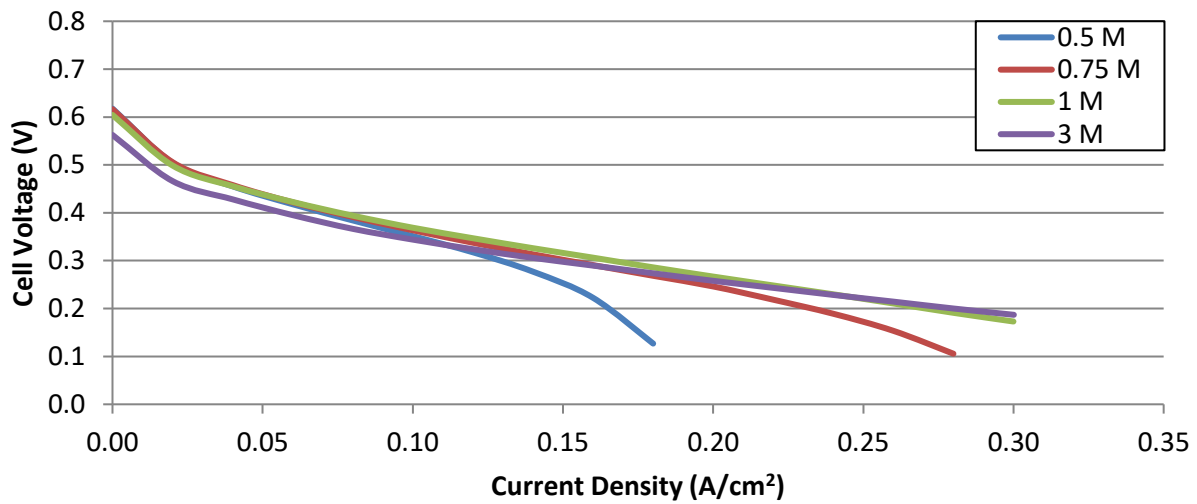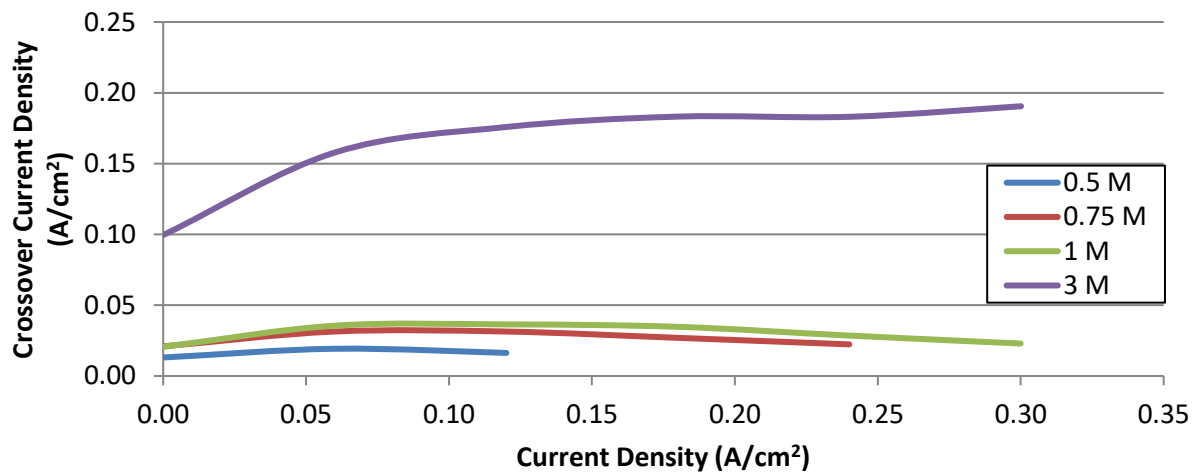

(a)

(b)

Fig. 10. (a) Polarization curve and (b) crossover current density of DMFC having a double N212 membrane at different methanol concentrations (0.5 M, 0.75 M, 1 M, and 3 M).

(a)

(b)

Fig. 11. (a) Polarization curve and (b) crossover current density of FE-DMFC based on N212 membranes at different methanol concentrations (0.5 M, 0.75 M, 1 M, and 3 M).

The trends for the change of crossover current density with respect to cell current density are found to be different for some of the methanol concentrations. For example, Fig. 8b shows that as the cell current density increases from 0 A/cm² to 0.18 A/cm², the crossover current density decreases from 0.040 A/cm² to 0.015 A/cm², 0.064 A/cm² to 0.040 A/cm², and 0.085 A/cm² to 0.065 A/cm² at 0.5 M, 0.75 M and 1 M, respectively, for a D-DMFC having a N115. However, for the 3 M case and the same cell current density change, the crossover current density first slowly and then sharply increases from 0.274 A/cm² to 0.287

A/cm^2. This finding can be explained as follows. Methanol crossover through the membrane mainly occurs due to diffusion and electro-osmosis mechanisms. An increase in the current density increases the methanol crossover due to electro-osmosis but reduces that due to diffusion because methanol concentration at the membrane surface is reduced by methanol consumption [24]. It can be interpreted that the reduction in methanol crossover due to diffusion is more influential than the increase due to electro-osmosis for low methanol concentrations (0.5 M, 0.75 M, and 1 M) and the opposite is correct for high methanol concentrations (3 M). In the case of the D-DMFC having a N212, the trends for crossover current density at 0.5 M, 0.75 M, and 1 M change in a similar way to D-DMFC having N115. At 3 M, it can be followed from Fig. 10b that the crossover current density first increases, then becomes almost constant, and starts decreasing at higher current densities. This trend might show that methanol crossover due to diffusion is nearly constant at low current densities, whereas the effect of crossover due to electro-osmotic drag would be more pronounced. As the current density increases, the surface concentration at the anode catalyst layer surface decreases, causing a decrease in both the diffusive and electro-osmotic fluxes. In the case of FE-DMFC, in addition to the aforementioned mechanisms, convection and diffusion mechanisms at the FEC are also influential. However, the primary difference with this configuration is the methanol removal by the FEC through convection. This allows for very low methanol surface concentrations at the cathode membrane - FEC interface, which translates to very low permeation rates to the cathode. Furthermore, since the concentration values are so low, this allows for the electro-osmotic drag mechanism to dominate, as was observed by the increasing crossover current density, with increase current density, such as in Figs. 9b and 11b. However, a decrease in crossover current density was observed at lower concentrations and higher current densities, due to the increased methanol consumption and low surface concentrations at the anode catalyst layer; causing the parabolic-like crossover current density profiles in each of the presented curves. This behavior would also be expected to occur for the higher feed concentrations (e.g. 3M), at higher current densities; due to the greater availability of reactants in the anode. However, it seems that the losses caused by the activation and Ohmic polarizations prevented this observation.

An important finding was that a Faradaic efficiency of 98 % (assuming that the methanol at the FEC outlet is reusable) was achieved at several cases. The following cell current densities (i) and crossover current densities (i_{xover}), which are given for the N115 based FE-DMFC (Fig. 9b), can be given as examples to these cases: 0.002 A/cm^2 (i_{xover}) at 0.12 A/cm^2 (i) at 0.5 M, 0.004 A/cm^2 (i_{xover}) at 0.18 A/cm^2 (i) at 0.75 M, and 0.0059 A/cm^2 (i_{xover}) at 0.3 A/cm^2 (i) at 1 M. This value of Faradaic efficiency is much higher than that what could be achieved in a conventional DMFC as methanol crossover would decrease this efficiency significantly. The maximum power density among all the studies conducted for the FE-DMFCs was achieved as 0.0561 W/cm^2 (for N212 based FE-DMFC operating with 3 M methanol concentration at 0.3 A/cm^2), which can be seen from Fig. 11a.

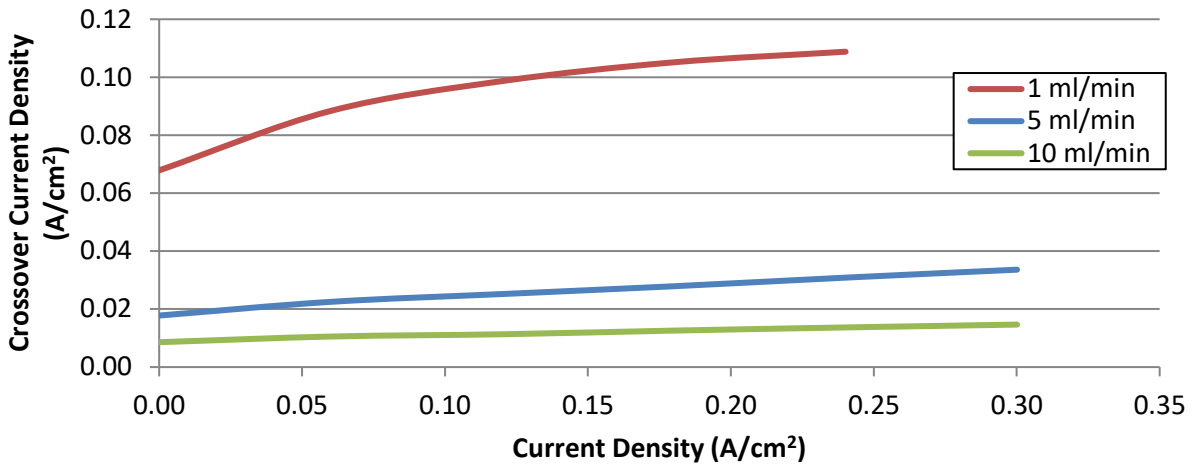### 3.4. Effect of Flow Rate of Sulfuric Acid Solution

One of the main parameters that have a significant impact on the performance of a FE-DMFC is the flow rate of the sulfuric acid solution. Previous numerical studies on the FE-DMFC (e.g. [24]) showed that this

parameter should be selected high enough to carry away the unwanted methanol crossover through convection mechanisms. It was also discussed that selecting this parameter too high means higher work input to the pump, which will reduce the overall electrical efficiency of a FE-DMFC system. On the other hand, the findings discussed in the previous subsections showed that when the methanol concentration is taken as 3 M and the flowing electrolyte flow rate is chosen as 5 ml/min, there is a potential for further performance gain with increasing the flow rate of sulfuric acid solution as the crossover current density was the highest for this case for a FE-DMFC. Hence, different values for the flow rate of sulfuric acid solution (1 ml/min, 5 ml/min, and 10 ml/min) were taken to discuss the effect of this flow rate on the performance of a FE-DMFC.

Figures 12a and 12b show the polarization curve and crossover current density for a FE-DMFC having N115 membrane, respectively; whereas Figs. 13a and 13b show those for a FE-DMFC having N212 membrane, respectively. The cell voltages at 0.1 A/cm^2 for the FE-DMFCs based on these membranes are also shown in Table 1. For both of these fuel cells, it can be seen from these figures and table that increasing the flow rate of sulfuric acid solution yields better performance as the crossover current density reduces. For example, Fig. 12a shows that, when the cell current density is 0.1 A/cm^2 the cell voltage for FE-DMFC having N115 is 0.307 V, 0.345 V, and 0.356 V, for the flow rate of 1 ml/min, 5 ml/min, and 10 ml/min, respectively. The crossover current densities for these flow rates are found to be 0.095 A/cm^2, 0.024 A/cm^2, and 0.011 A/cm^2, respectively, as can be seen from Fig. 12b. Several tests were also done increasing the flow rate further than 10 ml/min; but the performance change was negligible. It should also be noted that if a proper way to separate the methanol from the flowing electrolyte channel outlet can be found, the electrical efficiency of the cell could be significantly improved [24].
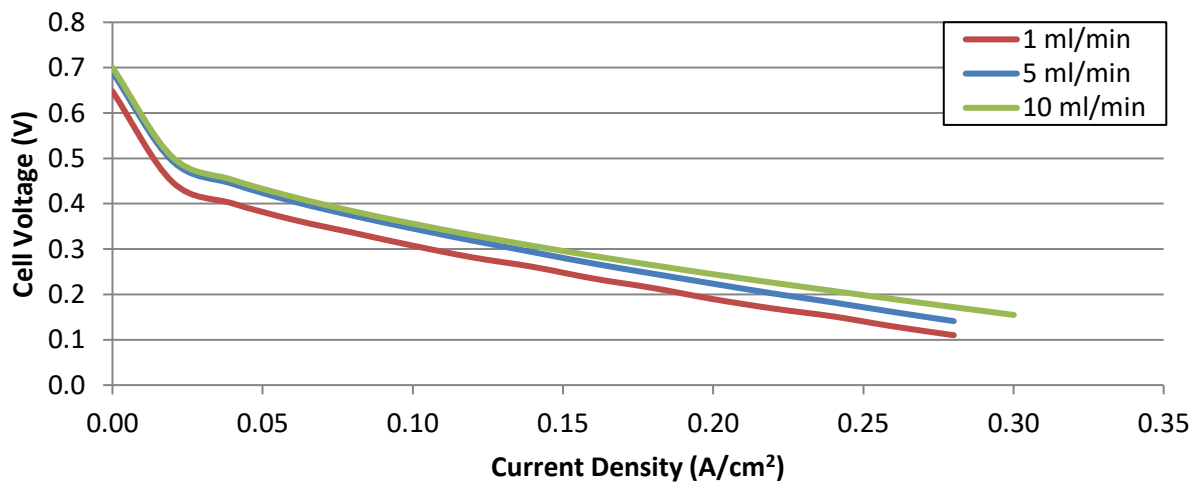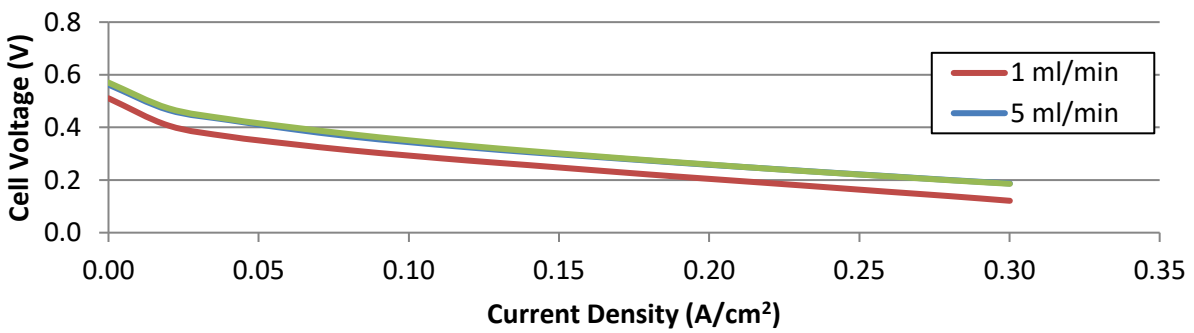

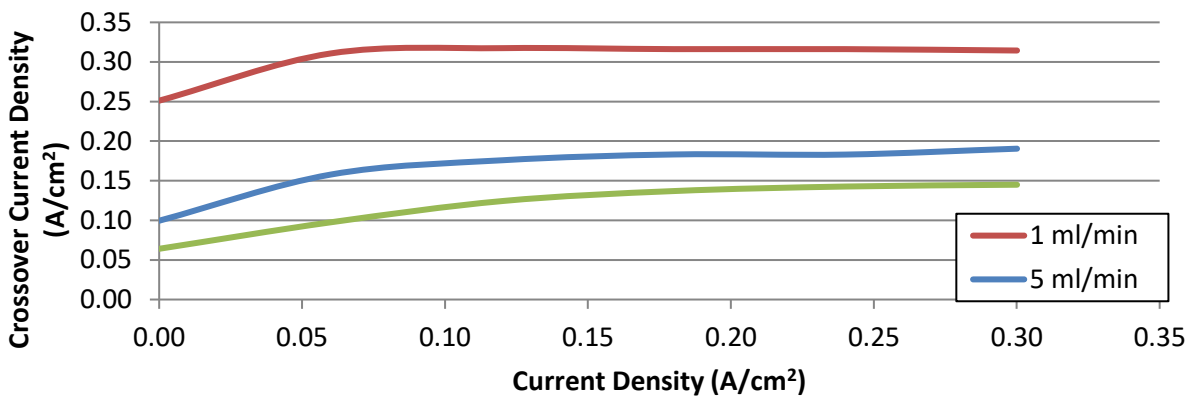**(a)**

(b)

Fig. 12. (a) Polarization curve and (b) crossover current density of FE-DMFC based on N115 membranes at different flow rates of sulfuric acid solution (1 ml/min, 5 ml/min, and 10 ml/min).

(a)

(b)

Fig. 13. (a) Polarization curve and (b) crossover current density of FE-DMFC based on N212 membranes at different flow rates of sulfuric acid solution (1 ml/min, 5 ml/min, and 10 ml/min).

4. Conclusions

In this study, FE-DMFCs having a new design and materials were manufactured and tested. In addition to FE-DMFCs, single and double membraned DMFCs were also manufactured for performance comparison purposes. N115 or N212 was used as the membrane; and the experiments were conducted at 70 °C for different values of methanol concentration (0.5 M, 0.75 M, 1 M, and 3 M) and sulfuric acid solution flow rate (1 ml/min, 5 ml/min, and 10 ml/min). Polarization curves and the change of methanol crossover density with cell current density were measured for each case. The main conclusions derived from this study can be listed as follows.

- The FE-DMFC can decrease the methanol crossover significantly. However, the performance is lower than DMFC due to higher Ohmic losses.
- High faradaic efficiencies up to 98 % are possible with the FE-DMFC at different current densities.
- Under the tested conditions, methanol crossover can be reduced by a factor of more than 10.
- Among the DMFCs having double membrane, the DMFC with N212 yielded the best performance (0.45 V at 0.1 A/cm^2) when it is fed with 0.5 M methanol concentration.
- Among the FE-DMFCs, the Nafion® 115 based fuel cell has the best performance (0.38 V at 0.1 A/cm^2) when it operates with 1 M methanol concentration and 5 ml/min sulfuric acid flow rate.
- The maximum power density of the FE-DMFC was achieved as 0.0561 W/cm^2 (for N212 based FE-DMFC operating with 3 M methanol concentration at 0.3 A/cm^2).
- If a FE-DMFC with a low membrane thickness (e.g. N212) operates at a high methanol concentration (e.g. 3 M) and sulfuric acid flow rate (e.g. 10 ml/min), the performance of that FE-DMFC gets closer to that of a DMFC having double membrane.

Using the new design and materials, much better performance (maximum power density of 0.0561 W/cm^2) was achieved for FE-DMFC compared to the previous experimental FE-DMFC studies (maximum power density of 0.035 W/cm^2 [29]) found in the literature. However, in order to compete with DMFCs, further development studies for FE-DMFCs should be conducted. These studies might include the effects of porous spacers with different thickness, porosity, and permeability, and higher methanol concentrations on the performance. Short-term and long-term degradation studies might be also conducted for FE-DMFCs made of flow field plates having higher corrosion resistances. On the other hand, the FE-DMFC could be considered as a characterization tool for studying the performance of cathodic electrodes and the influence of crossover in DMFCs.

References

1. Müller, M., Kimiaie, N., & Glüsen, A. (2014). Direct methanol fuel cell systems for backup power–Influence of the standby procedure on the lifetime. *International Journal of Hydrogen Energy*, *39*(36), 21739-21745.

2. Schirmer, J., Reissner, R., Zabold, J., Krajinovic, K., Häring, T., Nettesheim, S., Kopf. J., & Steinhart, K. (2011). BZ-BattExt–DMFC as Battery-Extender in solar-boat application. *Proceedings EFCF, 2011*.

3. Mergel, J., Janßen, H., Müller, M., Wilhelm, J., & Stolten, D. (2012). Development of Direct Methanol Fuel Cell Systems for Material Handling Applications. Journal of Fuel Cell Science and Technology, 9(3), 031011.

4. Zhao, T.S. & Xu, C. (2013). Direct Methanol Fuel Cell: Overview Performance and Operational Conditions. *Encyclopedia of electrochemical power sources*. C. K. Dyer, P. T. Moseley, Z. Ogumi, D. A. Rand, & B. Scrosati (Eds.). 381-389. Newnes.

5. Zawodzinski, T.A., Derouin, C., Radzinski, S., Sherman, R.J., Smith, V.T., Springer, T.E., & Gottesfeld, S. (1993), Water Uptake by and Transport Through Nafion® 117 Membranes. *Journal of the Electrochemical Society*, 140 (4) 1041-1047.

6. Ren, X.M., Henderson, W., & Gottesfeld, S. (1997) Electro-osmotic Drag of Water in Ionomeric Membranes New Measurements Employing a Direct Methanol Fuel Cell, *Journal of the Electrochemical Society*, 144 (9) L267-L270.

7. Ye, Q., & Zhao, T. S. (2005). Abrupt decline in the open-circuit voltage of direct methanol fuel cells at critical oxygen feed rate. *Journal of The Electrochemical Society*, *152*(11), A2238-A2245.

8. Walker, M., Baumgartner, K.M., Feichtinger, J., Kaiser, M., Rauchle, E., & Kerres, J. (1999) Barrier properties of plasma-polymerized thin films, *Surface & Coatings Technology*, 119 (116) 996-1000.

9. Choi, W. C., Kim, J. D., & Woo, S. I. (2001). Modification of proton conducting membrane for reducing methanol crossover in a direct-methanol fuel cell. *Journal of Power Sources*, *96*(2), 411-414.

10. Lin, C.W., Lu, & Y.S. (2013), Highly ordered graphene oxide paper laminated with a Nafion membrane for direct methanol fuel cells, *Journal of Power Sources*, 237 (1) 187-194.

11. Holmes, S.M., Balakrishnan, P., Kalangi, V.S., Zhang, X., Lozada-Hidalgo, M., Ajayan, P.M., & Nair, R.R. (2016) 2D Crystals Significantly Enhance the Performance of a Working Fuel Cell, *Advanced Energy Materials*, (2016) 1601216-1601223.

12. Ponce, M.L., Prado, L., Ruffmann, B., Richau, K., Mohr, R., & Nunes, S.P. (2003), Reduction of methanol permeability in polyetherketone–heteropolyacid membranes, *Journal of Membrane Science*, 217 (1-2) 5-15.

13. Kim, Y. M., Park, K. W., Choi, J. H., Park, I. S., & Sung, Y. E. (2003). A Pd-impregnated nanocomposite Nafion membrane for use in high-concentration methanol fuel in DMFC. *Electrochemistry Communications*, *5*(7), 571-574.

14. Parthiban, V., Akula, S., Peera, S. G., Islam, N., & Sahu, A. K. (2015). Proton Conducting Nafion-Sulfonated Graphene Hybrid Membranes for Direct Methanol Fuel Cells with Reduced Methanol Crossover. *Energy & Fuels*, *30*(1), 725-734.

15. Gierke, T.D., Munn, G.E., & Wilson, F.C. (1981) The morphology in Nafion perfluorinated membrane products, as determined by wide- and small-angle x-ray studies, *Journal of Polymer Science Part B-Polymer Physics*, 19 (1) 1687-1704.

16. Kreuer, K.D. (2001) On the development of proton conducting polymer membranes for hydrogen and methanol fuel cells, *Journal of Membrane Science*, 185 (1) 29-39.

17. Li, Q., Chen, Y., Rowlett, J. R., McGrath, J. E., Mack, N. H., & Kim, Y. S. (2014). Controlled Disulfonated poly (arylene ether sulfone) multiblock copolymers for direct methanol fuel cells. *ACS applied materials & interfaces*, *6*(8), 5779-5788.

18. Kerres, J.A. (2001) Development of ionomer membranes for fuel cells, *Journal of Membrane Science*, 185 (1) 3-27.
.

19. Lufrano, F., Baglio, V., Staiti, P., Antonucci, V. & Arico, A. S. (2013). Performance analysis of polymer electrolyte membranes for direct methanol fuel cells. *Journal of Power Sources*, *243*, 519-534.

20. Kordesch, K., Gsellmann, J., & Cifrain, M. (2000, June). Fuel Cells with Circulating Electrolytes and Their Advantages for AFCs and DMFCs part 1: Alkaline Fuel Cells. In *Proc. Power Sources Conf. 39th* (pp. 108-09).

21. Kordesch, K., Hacker, V., & Bachhiesl, U. (2001). Direct methanol–air fuel cells with membranes plus circulating electrolyte. *Journal of Power Sources*, *96*(1), 200-203.

22. Schaffer, T., Hacker, V., & Besenhard, J. O. (2006). Innovative system designs for DMFC. *Journal of power sources*, *153*(2), 217-227.

23. Kjeang, E., Goldak, J., Golriz, M. R., Gu, J., James, D., & Kordesch, K. (2006). A parametric study of methanol crossover in a flowing electrolyte-direct methanol fuel cell. *Journal of Power Sources*, *153*(1), 89-99.

24. Colpan, C. O., Cruickshank, C. A., Matida, E., & Hamdullahpur, F. (2011). 1D modeling of a flowing electrolyte-direct methanol fuel cell. *Journal of Power Sources*, *196*(7), 3572-3582.

25. Colpan, C. O., Fung, A., & Hamdullahpur, F. (2012). 2D modeling of a flowing-electrolyte direct methanol fuel cell. *Journal of Power Sources*, *209*, 301-311.

26. Kablou, Y., Cruickshank, C. A., & Matida, E. (2015). Experimental Analysis of a Small-Scale Flowing Electrolyte–Direct Methanol Fuel Cell Stack. *Journal of Fuel Cell Science and Technology*, *12*(4), 041007.

27. Duivesteyn, E., Cruickshank, C. A., & Matida, E. (2013). Modelling of a porous flowing electrolyte layer in a flowing electrolyte direct-methanol fuel cell. *International Journal of Hydrogen Energy*, *38*(30), 13434-13442.

28. Duivesteyn, E., Cruickshank, C. A., & Matida, E. (2014). Nonisothermal Hydrodynamic Modeling of the Flowing Electrolyte Channel in a Flowing Electrolyte–Direct Methanol Fuel Cell. *Journal of Fuel Cell Science and Technology*, *11*(2), 021011.

29. Sabet-Sharghi, N., Cruickshank, C. A., Matida, E., & Hamdullahpur, F. (2013). Performance measurements of a single cell flowing electrolyte-direct methanol fuel cell (FE-DMFC). *Journal of Power Sources*, *230*, 194-200.

30. Ouellette, D., Cruickshank, C. A., & Matida, E. (2014). Experimental investigation on the performance of a formic acid electrolyte-direct methanol fuel cell. *Journal of Fuel Cell Science and Technology*, *11*(2), 021003.

31. Ouellette, D., Colpan, C. O., Matida, E., & Cruickshank, C. A. (2015). A single domain approach to modeling the multiphase flow within a flowing electrolyte–direct methanol fuel cell. *International Journal of Hydrogen Energy*, *40*(24), 7817-7828.

32. Ouellette, D., Colpan, C. O., Matida, E., Cruickshank, C. A., & Hamdullahpur, F. (2015). A comprehensive 1D model of a flowing electrolyte-direct methanol fuel cell with experimental validation. *International Journal of Energy Research*, *39*(1), 33-45.

33. Ouellette, D., Colpan, C. O., Cruickshank, C. A., & Matida, E. (2015). Parametric studies on the membrane arrangement and porous properties of the flowing electrolyte channel in a flowing electrolyte–direct methanol fuel cell. *International Journal of Hydrogen Energy*, *40*(24), 7732-7742.

34. Atacan, O. F., Ouellette, D., & Colpan, C. O. (2016). Two-dimensional multiphase non-isothermal modeling of a flowing electrolyte–direct methanol fuel cell. *International Journal of Hydrogen Energy*. (Published online – DOI: 10.1016/j.ijhydene.2016.06.214)

35. Outokumpu Stainless Steel & High Performance Alloys. Duplex Stainless Steel Brochure. 1-11.

36. NeoNickel. Alloy Performance Guide. 1-18.

37. Darling, H. E. (1964). Conductivity of Sulfuric Acid Solutions. *Journal of Chemical & Engineering Data*, *9*(3), 421-426.

38. Ling, J., & Savadogo, O. (2004). Comparison of methanol crossover among four types of Nafion membranes. *Journal of the Electrochemical Society*, 151(10), A1604-A1610.

39. Seo, S. H., & Lee, C. S. (2010). The effects of membrane thickness on the performance and impedance of the direct methanol fuel cell. *Proceedings of the Institution of Mechanical Engineers, Part C: Journal of Mechanical Engineering Science*, 224(10), 2211-2221.

40. Yan, J., Huang, X., Moore, H. D., Wang, C. Y., & Hickner, M. A. (2012). Transport properties and fuel cell performance of sulfonated poly (imide) proton exchange membranes. *International Journal of Hydrogen Energy*. 37(7), 6153-6160.